Updated July 31st, 2005

Chapter V MoM Approach to a Metal Antenna

Contents

5.1. Basis functions for a metal structure

The Rao-Wilton-Glisson (RWG) basis functions [1] on triangles are used in the present study. The basis function in Fig. 5.1 includes a pair of adjacent (not necessarily co-planar) triangles and resembles a small spatial dipole with linear current distribution where each triangle is associated with either positive or negative charge.

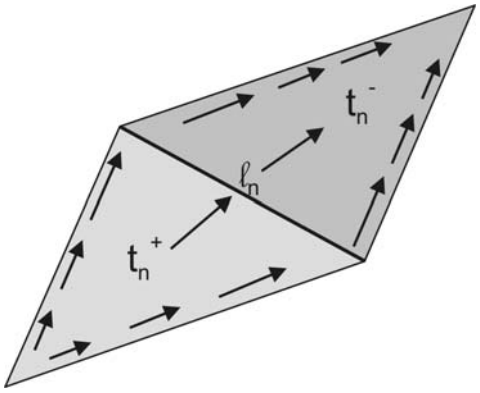

Fig. 5.1. RWG basis with two adjacent triangles [1].

Below, we recall some properties of the most common basis functions. For any two triangular patches, t_n^+ and t_n^-, having areas A_n^+ and A_n^-, and sharing a common edge l_n, the basis function becomes

$$\vec{f}_n^M(\vec{r}) = \begin{cases} \dfrac{l_n}{2A_n^+}\vec{\rho}_n^+ & \vec{r} \text{ in } t_n^+ \\ \dfrac{l_n}{2A_n^-}\vec{\rho}_n^- & \vec{r} \text{ in } t_n^- \end{cases} \tag{5.1}$$

and

$$\nabla \cdot \vec{f}_n^M(\vec{r}) = \begin{cases} \dfrac{l_n}{A_n^+} & \vec{r} \text{ in } t_n^+ \\ -\dfrac{l_n}{A_n^-} & \vec{r} \text{ in } t_n^- \end{cases} \tag{5.2}$$

where $\vec{\rho}_n^+ = \vec{r} - \vec{r}_n^+$ is the vector drawn from the free vertex of triangle t_n^+ to the observation point $\vec{r}$; $\vec{\rho}_n^- = \vec{r}_n^- - \vec{r}$ is the vector drawn from the observation point to the free vertex of triangle t_n^-. The basis function is zero outside the two adjacent triangles t_n^+ and t_n^-. The RWG vector basis function is linear and has no flux (that is, has no normal component) through its boundary.

5.2. MoM equations for a metal structure

a. Scattering problem

Scattering or radiation problems are essentially identical – the only difference is that the "incident" field for the driven antenna is the applied electric field in the feed. Therefore, only the scattering problem is considered here. The total electric field is a combination of the incident field (labeled by superscript *i*) and the scattered field (labeled by superscript *s*), i.e.

$$\vec{E} = \vec{E}^i + \vec{E}^s \tag{5.3}$$

The incident electric field is either the incoming signal (scattering problem) or the excitation electric field in the antenna feed (radiation problem). The scattered electric field $\vec{E}^s$ is due to surface currents and free charges on the metal surface *S* (the so-called mixed-potential formulation) [2]

$$\vec{E}^s = -j\omega\vec{A}_M(\vec{r}) - \nabla\Phi_M(\vec{r}) \quad \vec{r} \text{ on } S \tag{5.4}$$

Herein the index *M* denotes the metal-surface related quantities. The magnetic vector potential $\vec{A}_M(\vec{r})$ describes surface current radiation whereas the electric potential $\Phi_M(\vec{r})$ describes radiation of surface free charges. In the far field, both the Φ-contribution and the $\vec{A}$-contribution are equally important. On the metal surface *S*, the tangential component of the total electric field vanishes, $\vec{E}_{\tan} = 0$, thus giving the electric field integral equations (EFIE) [1, 2]

$$E^i_{\tan} = \left(j\omega \vec{\mathrm{A}}_M + \nabla \Phi_M \right)_{\tan} \quad \vec{r} \text{ on } S \tag{5.5}$$

b. Test functions

Assume that the test functions, $\vec{f}_m^{\,M}(\vec{r})$ $m = 1 \ldots N_M$, cover the entire surface S and do not have a component normal to the surface. Multiplication of Eq. (5.5) by $\vec{f}_m^{\,S}$ and integration over S gives N_M equations

$$\int_S \vec{f}_m^{\,M} \cdot \vec{E}^i ds = j\omega \int_S \vec{f}_m^{\,M} \cdot \vec{A}_M ds - \int_S \left(\nabla \cdot \vec{f}_m^{\,M} \right) \Phi_M ds \tag{5.6}$$

since, according to the Stokes theorem,

$$\int_S \nabla \Phi_M \cdot \vec{f}_m^{\,M} ds = -\int_S \Phi_M \left(\nabla \cdot \vec{f}_m^{\,M} \right) ds \tag{5.7}$$

if $\vec{f}_m^{\,M}$ does not have a component perpendicular to the surface boundary or edge (if any).

c. Source functions

The surface current density, $\vec{J}_M$ is expanded into the basis functions (which usually coincide with the test functions) in the form

$$\vec{J}_M = \sum_{n=1}^{N_M} I_n \vec{f}_n^{\,M} \tag{5.8}$$

The magnetic vector potential has the form [2]

$$\vec{\mathrm{A}}_M(\vec{r}) = \frac{\mu_0}{4\pi} \int_S \vec{J}_M g ds' \tag{5.9}$$

where μ_0 is the permeability in vacuum and $g = \exp(-jkR)/R, R = \left| \vec{r} - \vec{r}' \right|$ is the free-space Green's function (time dependency $\exp(j\omega t)$ is assumed everywhere). In the expression for the Green's function $\vec{r}$ is the observation (test) point and $\vec{r}'$ is the

integration (source) point; both of them belong to the metal surface. After substitution of the expansion Eq. (5.8), the above equation becomes

$$\vec{A}_M(\vec{r}) = \sum_{n=1}^{N_M} \left\{ \frac{\mu_0}{4\pi} \int_S \vec{f}_n^{\,M}(\vec{r}\,')g ds' \right\} I_n \tag{5.10}$$

Similarly, the electric potential has the form [2]

$$\Phi_M(\vec{r}) = \frac{1}{4\pi\varepsilon_0} \int_S \sigma_M g ds', \quad j\omega\sigma_M = -\nabla_S \cdot \vec{J}_M \tag{5.11}$$

It follows from equation (5.11) that σ_s can be expressed in terms of the current density, through the surface divergence. Hence the electric vector potential reduces to

$$\Phi_M(\vec{r}) = \sum_{n=1}^{N_M} \left\{ \frac{1}{4\pi\varepsilon_0} \frac{j}{\omega} \int_S \nabla \cdot \vec{f}_n^{\,M}(\vec{r}\,')ds' \right\} I_n \tag{5.12}$$

d. Moment equations

The moment equations are obtained if we substitute expansions (5.10) and (5.12) into the integral equation (5.6). In terms of symbolic notations,

$$\sum_{n=1}^{N_M} \hat{Z}_{mn}^{MM} I_n = \upsilon_m^M, \quad m = 1,..., N_M \tag{5.13}$$

where

$$\upsilon_m^M = \int_S \vec{f}_m^{\,M} \cdot \vec{E}^i ds \tag{5.14}$$

are the "voltage" or excitation components for every test/basis function that have units V·m. The integral expressions are the components of the impedance matrix $\hat{Z}^{MM}$ of size (N_M x N_M),

$$Z_{mn}^{MM} = \left(\frac{j\omega\mu_0}{4\pi}\right)\int_S\int_S \vec{f}_m^{\,M}(\vec{r})\cdot\vec{f}_n^{\,M}(\vec{r}\,')gds'ds - \left(\frac{j}{4\pi\omega\varepsilon_0}\right)\int_S\int_S\left(\nabla\cdot\vec{f}_m^{\,M}\right)\left(\nabla\cdot\vec{f}_n^{\,M}\right)gds'ds \qquad (5.15)$$

Note that the impedance matrix is symmetric for any set of basis functions (test functions should be the same) when the corresponding surface integrals are calculated precisely. The components of the impedance matrix are the double surface integrals of the Green's function and they mostly reflect the geometrical interaction between the "dipole" RWG basis functions of the problem. In matrix form, Eq. (5.15) becomes

$$\hat{Z}^{MM}\vec{I} = \vec{\upsilon} \qquad (5.16)$$

Substitution of Eqs. (5.1), (5.2) into Eq. (5.15) gives the components of the impedance matrix in terms of surface RWG basis functions in the form

$$\begin{aligned}
&\int_S\int_S \vec{f}_m^{\,M}\cdot\vec{f}_n^{\,M}\,gds'ds = \\
&+\frac{l_m l_n}{4A_m^+A_n^+}\int_{t_m^+}\int_{t_n^+}\left(\vec{\rho}_m^{\,+}\cdot\vec{\rho}_n^{\,\prime+}\right)gds'ds + \frac{l_m l_n}{4A_m^+A_n^-}\int_{t_m^+}\int_{t_n^-}\left(\vec{\rho}_m^{\,+}\cdot\vec{\rho}_n^{\,\prime-}\right)gds'ds \\
&+\frac{l_m l_n}{4A_m^-A_n^+}\int_{t_m^-}\int_{t_n^+}\left(\vec{\rho}_m^{\,-}\cdot\vec{\rho}_n^{\,\prime+}\right)gds'ds + \frac{l_m l_n}{4A_m^-A_n^-}\int_{t_m^-}\int_{t_n^-}\left(\vec{\rho}_m^{\,-}\cdot\vec{\rho}_n^{\,\prime-}\right)gds'ds
\end{aligned} \qquad (5.17)$$

and

$$\begin{aligned}
&\int_S\int_S\left(\nabla\cdot\vec{f}_m^{\,M}\right)\left(\nabla\cdot\vec{f}_n^{\,M}\right)gds'ds = \\
&+\frac{l_m l_n}{A_m^+A_n^+}\int_{t_m^+}\int_{t_n^+} gds'ds - \frac{l_m l_n}{A_m^+A_n^-}\int_{t_m^+}\int_{t_n^-} gds'ds \\
&-\frac{l_m l_n}{A_m^-A_n^+}\int_{t_m^-}\int_{t_n^+} gds'ds + \frac{l_m l_n}{A_m^-A_n^-}\int_{t_m^-}\int_{t_n^-} gds'ds
\end{aligned} \qquad (5.18)$$

5.3. Integral calculation

a. Base integrals

About 90% of the CPU time required for the filling of the MoM impedance matrix $\hat{Z}^{MM}$ for the RWG basis functions is spent for the calculation of the surface integrals presented in equations (5.17), (5.18). Consider a structure where all triangular patches are enumerated by $p = 1,..., P$. Then, every integral in equation (5.17) is built upon the term

$$\vec{A}^{ij}_{M\,pq} = \int_{t_p}\int_{t_q} \left(\vec{\rho}_i \cdot \vec{\rho}'_j\right) g(|\vec{r} - \vec{r}\,'|) ds' ds \quad p, q = 1,..., P \quad i, j = 1,2,3 \tag{5.19}$$

Here, $\vec{\rho}_i = \vec{r} - \vec{r}_i$ for any vertex *i* of patch *p* whereas $\vec{\rho}'_j = \vec{r}\,' - \vec{r}_j$ for any vertex *j* of patch *q*. Similarly, every integral in equation (5.18) is built upon the term

$$\Phi_{M\,pq} = \int_{t_p}\int_{t_q} g(|\vec{r} - \vec{r}\,'|) ds' ds \quad p, q = 1,..., P \tag{5.20}$$

The integrals (5.19) and (5.20) can be found in a number of ways.

b. Singularity extraction

The singularity of the free-space Green's function is integrable in 2D, but the accuracy of the Gaussian formulas is reduced if this singularity is retained. Therefore, singularity extraction may be used in Eqs. (5.19), (5.20), in the form

$$\int_{t_p}\int_{t_q} \left(\vec{\rho}_i \cdot \vec{\rho}'_j\right) g(|\vec{r} - \vec{r}\,'|) ds' ds = \int_{t_p}\int_{t_q} \frac{\left(\vec{\rho}_i \cdot \vec{\rho}'_j\right)}{|\vec{r} - \vec{r}\,'|} ds' ds + \int_{t_p}\int_{t_q} \frac{\left(\exp(-jk|\vec{r} - \vec{r}\,'|) - 1\right)\left(\vec{\rho}_i \cdot \vec{\rho}'_j\right)}{|\vec{r} - \vec{r}\,'|} ds' ds \tag{5.21}$$

$$\int_{t_p}\int_{t_q} g(|\vec{r} - \vec{r}\,'|) ds' ds = \int_{t_p}\int_{t_q} \frac{1}{|\vec{r} - \vec{r}\,'|} ds' ds + \int_{t_p}\int_{t_q} \frac{\left(\exp(-jk|\vec{r} - \vec{r}\,'|) - 1\right)}{|\vec{r} - \vec{r}\,'|} ds' ds \tag{5.22}$$

The two first singular integrals on the right-hand side of Eqs. (5.21), (5.22) (the so-called potential or static integrals) may be found with the help of the analytical results given in [3]. The double self-integrals are evaluated analytically in [4].

c. Analytical calculation of potential integrals [3]

Strictly speaking, the integration-by-parts approach of Ref. [3] allows us only to find the inner potential integral presented in Eqs. (5.21), (5.22). The outer integrals will still be found numerically, using the Gaussian cubatures [5]. Fig. 5.2, which is given for one triangle edge and the observation point, is useful in visualizing many variables needed to find the potential integrals using the analytic formulas. This figure and the corresponding integration formulas are adopted from Ref. [3]. Here, $\vec{\rho}$ is the projection vector of the observation point $\vec{r}$ onto the triangle plane, $\vec{\rho}'$ is the projection vector of the integration point $\vec{r}'$ onto the triangle plane, and R is the distance between the integration point and the observation point, i.e. $R = \left| \vec{r}' - \vec{r} \right|$.

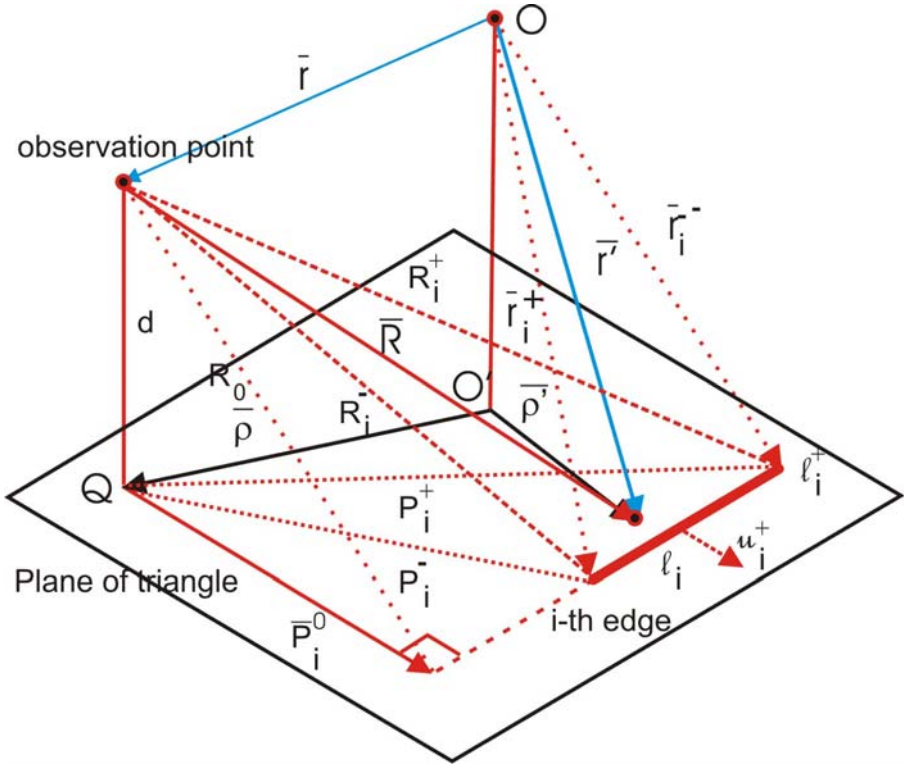

Fig. 5.2. Geometric representation of the variables in the analytical formulas [3] (© 1984 IEEE).

Below, we briefly review the related results of [3]. The analytic formula for the inner (potential) integral on the right-hand side of Eq. (5.22) has the following form:

$$\int_{t_q} \frac{1}{|\vec{r}-\vec{r}'|}\, ds' =$$
$$-\alpha(\vec{\rho})\,|d| + \sum_{i=1}^{3} \vec{P}_i^{\,0} \cdot \vec{u}_i \left[\mathrm{P}_i^0 \ln \frac{R_i^+ + l_i^+}{R_i^- + l_i^-} + |\,d\,| \left(\tan^{-1} \frac{|\,d\,|\, l_i^+}{\mathrm{P}_i^0 R_i^+} - \tan^{-1} \frac{|\,d\,|\, l_i^-}{\mathrm{P}_i^0 R_i^-} \right) \right] \tag{5.23}$$

The summation is made over the three edges of the triangle. Here, $\alpha(\vec{\rho})$ is the angle factor and is either 0 or 2π depending on whether the projection of the observation point is outside the triangle or inside the triangle, respectively. The quantity d is the height of the observation point above the plane of triangle *t*, measured positively in the direction of the triangle normal vector $\vec{n}$. The quantity *d* is calculated by $d = \vec{n} \cdot (\vec{r} - \vec{r}_i^{\,+})$, where $\vec{r}_i^{\,+}$ is a given position vector to the "upper" endpoint of edge l_i, $i = 1,2,3$. The upper endpoint is labeled with symbol "+". Triangle unit normal $\vec{n}$ is the cross product of side 1 and side 2 vectors of the triangle, where numbering the sides is arbitrary as long as it is consistent for each iteration of the formula. Alternatively, $\vec{r}_i^{\,-}$, a given position vector to the "lower" endpoint of edge l_i, $i = 1,2,3$, can be used in the equation for *d* instead of $\vec{r}_i^{\,+}$. The perpendicular vector from the endpoint of vector $\vec{\rho}$ in Fig. 5.2 to the edge l_i, $i = 1,2,3$ or its extension is given by $\vec{\mathrm{P}}_i^{\,0} = \dfrac{(\vec{\rho}_i^{\,\pm} - \vec{\rho}) - (l_i^{\,\pm} \vec{l}_i)}{\mathrm{P}_i^{\,0}}$, where $\vec{\rho}_i^{\,\pm}$ are the vectors from point *Q* to the endpoints of the edge, which are equal to $\vec{r}_i^{\,\pm} - \vec{n}\,(\vec{n} \cdot \vec{r}_i^{\,\pm})$. $\vec{l}_i$ is the edge vector and is equal to $\dfrac{\vec{r}_i^{\,+} - \vec{r}_i^{\,-}}{\left| \vec{r}_i^{\,+} - \vec{r}_i^{\,-} \right|}$ (see Fig. 5.2). The endpoints of $\vec{l}_i$ are associated with distances $l_i^{\,\pm} = (\vec{\rho}_i^{\,\pm} - \vec{\rho}) \cdot \vec{l}_i$ (see Fig. 5.2). The distance from the endpoint of vector $\vec{\rho}$ in Fig. 5.2 to the edge l_i, $i = 1,2,3$ or its extension is given by $\mathrm{P}_i^0 = \left| (\vec{\rho}^{\,\pm} - \vec{\rho}) \cdot \vec{u}_i \right|$ (the proper sign must be taken into account). The vector $\vec{u}_i$ is the unit outer normal to the edge and is equal to $\vec{l}_i \times \vec{n}$. Distances measured from $\vec{\rho}$ to $\vec{\rho}_i^{\,\pm}$ are $\mathrm{P}_i^{\,\pm} = \left| \vec{\rho}_i^{\,\pm} - \vec{\rho} \right| = \sqrt{\left(\mathrm{P}_i^{\,0} \right)^2 + \left(l_i^{\,\pm} \right)^2}$. The two quantities $R_i^{\pm} = \sqrt{\left(\mathrm{P}_i^{\pm} \right)^2 + d^2}$ are the distances measured from the observation point to the endpoints of the edge (see Fig. 5.2). This completes the list of variables presented in Eq. (1.5).

The inner integral in Eq. (5.21) is similar to that in Eq. (5.22) except that it is multiplied by $\vec{\rho}_j'$. This gives a vector-valued integral. The corresponding analytic formula given in [3] provides the integral

$$\int_{t_q} \frac{(\vec{r}'-r)_{\tan}}{|\vec{r}-\vec{r}'|}\,ds' = \frac{1}{2}\sum_{i=1}^{3} \vec{u}_i \left[\left(R_i^0\right)^2 \ln \frac{R_i^+ + l_i^+}{R_i^- + l_i^-} + l_i^+ R_i^+ - l_i^- R_i^- \right] \tag{5.24}$$

where subscript *tan* denotes the vector projection onto the triangle plane, $R_i^0 = \sqrt{\left(\mathrm{P}_i^0\right)^2 + d^2}$ is the distance measured from the observation point to the point intersected by $\vec{\mathrm{P}}_i^0$ and $\vec{l}$. The remaining variables are the same as in Eq. (5.23). The inner integral on the right-hand-side of Eq. (5.21) is then obtained as a combination of (5.23) and (5.24), i.e.,

$$\int_t \frac{\rho_j'}{|\vec{r}-\vec{r}'|}\,ds' = \int_t \frac{(\vec{r}'-r)_{\tan}}{|\vec{r}-\vec{r}'|}ds' + \left(\vec{r}-\vec{r}_j\right)_{\tan} \int_t \frac{1}{|\vec{r}-\vec{r}'|}\,ds' \tag{5.25}$$

5.4. Fields

a. Scattered electric field

Once the MoM solution is known, the scattered (or radiated) electric field is given by Eq. (5.4)

$$\begin{aligned} \vec{E}^s = & \frac{-j\omega\mu_0}{4\pi} \sum_{n=1}^{N_M} \left\{ \int_S \vec{f}_n{}^M(\vec{r}')\, g(\vec{r},\vec{r}')\, ds' \right\} I_n \\ & - \frac{j}{4\pi\omega\varepsilon_0} \sum_{n=1}^{N_M} \left\{ \int_S \nabla\cdot \vec{f}_n^{\,M}(r')\, \nabla_r g(\vec{r},\vec{r}')\, ds' \right\} I_n \end{aligned} \tag{5.26}$$

where I_n is the MoM solution for surface current density.

a. Scattered magnetic field

The scattered magnetic field created by a metal structure is given by the curl of the magnetic vector potential, i.e.

$$\vec{H}^s = \frac{1}{4\pi}\int_S \sum_{n=1}^{N_M} \left\{ \left(-\vec{f}_n^{\,M}(\vec{r}\,') \times \nabla_r g(\vec{r},\vec{r}\,') \right) ds' \right\} I_n \tag{5.27}$$

5.5. Method of calculation of the impedance matrix $\hat{Z}^{MM}$ and the radiated/scattered fields

a. Impedance matrix

A "neighboring" sphere of dimensionless radius R is introduced for every integration facet. The radius R is a threshold value for the ratio of distance to size. The size of the facet t_q, $S(t_q)$, is measured as the distance from its center to the furthest vertex. The observation triangle t_p lies within the sphere if the following inequality is valid for the distance d between two triangle centers

$$\frac{d}{\sqrt{S(t_p)S(t_q)}} < R \tag{5.28}$$

If a pair of triangles satisfies (5.28), then the integrals (5.19) and (5.20) use the singularity extraction (5.21), (5.22) and the analytical formulas (5.23)-(5.25) for the inner potential integrals. The non-singular part and the outer potential integrals employ Gaussian cubatures given in [5]. Each cubature is characterized by two numbers: N, the number of integration points; and d, the degree of accuracy for the Gaussian cubature formula. If a pair of triangles does not satisfy Eq. (5.28), then the central-point approximation is used for all integrals, without singularity extraction.

The parameter R is initialized in the script `metal.m` in subfolder `2_basis\codes`. The same is valid for N and d for the Gaussian formulas. The default values are $R = \sqrt{5}$ and $N = 3, d = 2$. The necessary potential integrals on the right-hand

sides of Eqs. (5.21), (5.22) are pre-calculated in structure *geom* and are saved in the sparse matrix format.

b. Fields

The same operation as for the impedance matrix is done for the field integrals (5.26) and (5.27) but Eq. (5.28) is now replaced by

$$\frac{d}{S(t_q)} < R \tag{5.28}$$

Within the sphere, one more potential integral appears, of the form [6]

$$\int_S \nabla \frac{1}{|\vec{r} - \vec{r}\,'|}\, ds = -\vec{n} \cdot \mathrm{sgn}(d) \cdot \beta - \sum_{i=1}^{3} \vec{u}_i \ln \frac{R_i^+ + l_i^+}{R_i^- + l_i^-} \tag{5.29}$$

where

$$\beta = \sum_{i=1}^{3} \left[\tan^{-1} \frac{\mathrm{P}_i^0 l_i^+}{\left(R_i^0\right)^2 + |d| R_i^+} - \tan^{-1} \frac{\mathrm{P}_i^0 l_i^-}{\left(R_i^0\right)^2 + |d| R_i^-} \right] \tag{5.30}$$

and the variables are the same as in Eqs. (5.23) and (5.24).

The parameter R is initialized in the script `field.m` in subfolder `3_mom\codes`. The default value is $R = 2$. The N and d for the Gaussian formula are defined as $N = 7, d = 5$ in the script `fieldm.cpp`. Outside the sphere, the central-point approximation is used. For the far-field approximation, $R \to 0$ is an acceptable approximation.

5.6. List of available Gaussian integration formulas on triangles

Some Gaussian integration formulas on triangles [5] are given in the script `tri.m` in subfolder `2_basis\codes.` The formulas given in Table 5.1 were used and tested. Each cubature is characterized by two numbers: N is the number of integration points and d is the degree of accuracy for the Gaussian cubature formula.

Table 5.1. List of available/tested Gaussian formulas on triangles [5].

Formula	N	d
#1	1	1
#2	3	2
#3	4	3
#4	6	3
#5	7	5
#6	9	5
#7	13	7
#8	25	10

Also, the barycentric triangle subdivision of arbitrary degree of subdivision is available in the script `tri.m`.

5.7. Summary of numerical operations and associated MATLAB/C++ scripts

The summary of numerical operations related to a metal antenna/resonator/scatterer is given in Table. 5.2. The same summary but for a metal resonator is given in Table 5.3. The difference between the two cases is mostly in the antenna feed.

Table 5.2. Antenna-related numerical operations.

Antenna operations			
Operation	Script	Path	Remarks
Determine the metal structure	`struct2d.m` `struct3d.m`	`1_mesh`	Remove all tetrahedra from the mesh while running `struct3d.m`. Do not use $\varepsilon_r = 1$.
Determine the antenna feed location	`feed.m` (obsolete; combined with `struct3d`)	`1_mesh`	The feed edges are found as the closest ones to the array `POINTS`. The number of feeding edges in the feed can be arbitrary.
Determine parameters of the RWG basis functions	`wrapper.m`	`2_basis`	Outputs structure `geom` with all the necessary data on the basis functions/precalculated potential integrals
Determine accuracy of impedance matrix filling – optional	`metal.m`	`2_basis\codes`	The parameter R is initialized in the script `metal.m` in subfolder `2_basis\codes`. The same is

(see Section 5.5)			valid for *N* and *d* for the Gaussian formulas. The default values are $R=\sqrt{5}$ and $N=3, d=2$. The necessary potential integrals are pre-calculated in structure `geom` and are saved in the sparse matrix format.
Determine the antenna feed type	`impedance.m`	`3_mom`	Voltage gap is the default. Can be modified if necessary.
Determine the antenna input impedance and feed power (loop)	`impedance.m`	`3_mom`	Saves MoM solutions obtained at every frequency step in `out.mat`.
Determine radiation patterns (co-polar/cross-polar polarization, RHCP, LHCP)	`radpattern.m`	`3_mom`	Should be run after `impedance.m`. `Radpattern.m` uses the MoM solution obtained previously in order to compute the far fields. `Radpattern.m` finds the far field at a given frequency that needs to be specified.
Determine charge/current distribution on the metal surface	`nearfield.m`	`3_mom`	Should be run after `impedance.m`. `nearfield.m` uses the MoM solution obtained previously in order to compute the current/charge distributions at a given frequency (which needs to be specified).

Table 5.3. Resonator-related numerical operations. The feed (or feed column) does not have to be specified.

Resonator operations			
Operation	Script	Path	Remarks
Determine the metal structure	`struct2d.m` `struct3d.m`	`1_mesh`	Remove all tetrahedra from the mesh while running `struct3d.m`. Do not use $\varepsilon_r = 1$.
Determine parameters of RWG basis functions	`wrapper.m`	`2_basis`	Outputs structure `geom` with all necessary data on the basis functions/precalculated potential integrals
Determine accuracy of impedance matrix filling –optional	`metal.m`	`2_basis\ codes`	The parameter *R* is initialized in the script `metal.m` in subfolder `2_basis\codes`. The same is

(see Section 5.5)			valid for *N* and *d* for the Gaussian formulas. The default values are $R = \sqrt{5}$ and $N = 3, d = 2$. The necessary potential integrals are pre-calculated in structure *geom* and are saved in the sparse matrix format.
Determine eigenfrequency/Q-factor	`eigenfreq.m`	`3_mom`	Fully interactive interface. Will not run if the antenna feed is specified.
Determine charge/current distribution on the metal surface in the resonant mode	`scatterfield.m`	`3_mom`	Should be run after `eigenfreq.m`. `scatterfield.m`. Illuminates the resonator by an incident plane wave at the resonant frequency and finds the current/charge distributions at that given frequency

The independent scattering problem may be also considered, by running `scatterfield.m` at a given frequency.

References

1. S. M. Rao, D. R. Wilton, and A. W. Glisson, "Electromagnetic scattering by surfaces of arbitrary shape," *IEEE Trans. Antennas and Propagation*, vol. AP-30, no. 3, pp. 409-418, May 1982.
2. A. F. Peterson, S. L. Ray, and R. Mittra, *Computational Methods for Electromagnetics*, IEEE Press, Piscataway, New Jersey, 1998.
3. D. R. Wilton, S. M. Rao, A. W. Glisson, D. H. Schaubert, O. M. Al-Bundak, and C. M. Butler, "Potential integrals for uniform and linear source distribution on polygonal and polyhedral domains," *IEEE Trans. Antennas and Propagation*, vol. AP-32, no. 3, pp. 276-281, March 1984.
4. T. F. Eibert and V. Hansen, "On the calculation of potential integrals for linear source distributions on triangular domains," *IEEE Trans. Antennas and Propagation*, vol. AP-43, no. 12, pp. 1499-1502, Dec. 1995.
5. R. Cools, "An Encyclopedia of Cubature Formulas," *J. Complexity*, vol. 19, 445-453, 2003. Available onl.: http://www.cs.kuleuven.ac.be/~nines/research/ecf/ecf.html
6. Z. Wang, J. Volakis, K. Saitou, and K. Kurabayashi, "Comparison of semi-analytical formulations and Gaussian-quadrature rules for quasi-static double-surface potential integrals," *IEEE Antennas and Propagation Magazine*, vol. 45, no. 6, 2003, pp. 96-102.